Advanced Composite Materials
Publication details, including instructions for authors and subscription information:
http://www.tandfonline.com/loi/tacm20

Properties of vapor grown carbon nano fiber/phenylethynyl terminated polyimide composite

Toshio Ogasawara , Yuichi Ishida & Takashi Ishikawa
Version of record first published: 02 Apr 2012.

To cite this article: Toshio Ogasawara , Yuichi Ishida & Takashi Ishikawa (2004): Properties of vapor grown carbon nano fiber/phenylethynyl terminated polyimide composite, Advanced Composite Materials, 13:3-4, 215-226

To link to this article: http://dx.doi.org/10.1163/1568551042580208

Adv. Composite Mater., Vol. 13, No. 3-4, pp. 215–226 (2004)

Also available online - www.vsppub.com

Properties of vapor grown carbon nano fiber/phenylethynyl terminated polyimide composite

TOSHIO OGASAWARA *, YUICHI ISHIDA and TAKASHI ISHIKAWA

Institute of Space Technology and Aeronautics, Japan Aerospace Exploration Agency (JAXA), 6-13-1, Ohsawa, Mitaka-shi, Tokyo 181-0015, Japan

Received 12 April 2004; accepted 11 June 2004

Abstract—Vapor grown carbon nanofibers (VGCF) were dispersed throughout phenylethynyl terminated polyimide 'Triple A PI (TriA-PI)'. TriA-PI is a newly developed thermosetting polyimide, and the cured polymer exhibits excellent mechanical properties and high glass transition temperature ($T_g > 300°C$). The resulting composites containing 0, 3.2, 7.7, and 14.3 wt% of VGCFs exhibited relatively good dispersion in macroscopic observations. Dynamic mechanical analysis (DMA) showed an increase in T_g with incorporation of VGCFs; however, increase in T_g was not pronounced compared to multi-walled carbon nanotube (MWNT) dispersion. The experimental result suggested that the VGCFs and MWNT are immobilizing the polyimide chains at elevated temperature, and the chemical and physical interactions between nanofibers and the polyimide are governed by the surface area of the nanofibers per unit volume in composites.

Keywords: Polyimides; carbon nanotubes; carbon nanofibers; thermomechanical properties.

1. INTRODUCTION

Carbon nanofibers (CNFs), including single and multi-walled carbon nanotubes (CNTs), have a number of outstanding properties, so they are a very attractive reinforcement for polymer composites [1, 2]. There has been recent interest in the development of CNT/CNF based polymer composites. The effects of nanofiber dispersion on mechanical, thermal, and electrical properties have been investigated for various kinds of thermoplastic polymers such as polypropylene [3, 4], polystyrene (PS) [5], poly methyl methacrylate (PMMA) [6–8], nylon 12, poly etheretherketone (PEEK) [9], polycarbonate [10], etc., and increases in strength, elastic modulus, and electrical conductivity have been found. For thermosetting polymers, many researchers investigated the properties of CNT/epoxy composites, and increases in elastic modulus, electrical conductivity, and glass transition temperature

*To whom correspondence should be addressed. E-mail: ogasawara.toshio@jaxa.jp

(T_g) were reported [11–14]. On the other hand, there are few published papers regarding CNT/polyimide composites, e.g. SW-CNT/low color space durable polyimide 'LaRC™ CP2' composites for spacecraft application [15, 16].

The authors investigated processing and properties of multi-walled carbon nanotubes (MWNT)/thermosetting polyimide 'Tri-A PI' composites [17]. Tri-A PI is a new phenylethynyl terminated polyimide synthesized from asymmetric 2,3,3′,4′-biphenyltetracarboxylic dianhydride (a-BPDA), 4,4′-oxydianiline (4,4′-ODA), and 4-phenylethynylphthalic anhydride (PEPA) [18, 19]. The cured polymer exhibits excellent mechanical properties and high glass transition temperature ($T_g > 300°C$). Because of the catenation from the dianhydride, the Tri-A PI have highly irregular structures resulting in lower melting temperature, and the cured polymer exhibits high T_g in comparison to other kinds of phenylethynyl terminated polyimides such as PETI-5 ($T_g = 270°C$) [20]. Dynamic mechanical analysis (DMA) showed an increase in T_g with the incorporation of MWNTs, e.g. T_g increased by 24 deg (357°C) for a 14.3% MWNT dispersed composite [17]. The experimental result suggested that the MWNTs are acting as macroscopic crosslinks, and are further immobilizing the polyimide chains at elevated temperature.

Recently, Showa Denko KK (Tokyo, Japan) began to produce vapor grown carbon nanofibers (VGCF) on a large scale [21, 22]. Therefore, VGCFs can be obtained at a reasonable cost compared to MWNTs. The objective of this paper is to examine the effect of VGCF dispersion on the properties of thermosetting polyimide Tri-A PI. The composites containing 0, 3.2, 7.7, and 14.3 wt% of VGCFs were made, and the properties such as melt viscosity, dynamic mechanical behavior, and electrical resistance were characterized. The experimental results were directly compared to the MWNT/Tri-A PI composites.

2. EXPERIMENTAL

2.1. Starting materials

VGCFs used in this study were obtained from Showa Denko K.K. (Tokyo, Japan). VGCFs were synthesized by chemical vapor deposition (CVD) process. Figure 1a is an SEM micrograph showing the VGCFs. The diameter of the VGCF ranged from 150 to 200 nm, and the average length was a few micrometers. On the other hand, MWNTs used in the previous study were obtained from Carbon Nanotech Research Institute (CNRI) Inc, (Tokyo, Japan). An SEM micrograph is shown in Fig. 1b. The diameter of MWNTs was in the range of 20-80 nm, which was much smaller than that of VGCF. Both VGCF and MWNT are highly entangled and randomly oriented.

Tri-A PI imide oligomer was provided by UBE Industries Ltd. (Tokyo, Japan). The imide oligomer was synthesized from 4,4′-ODA, 2,3,3′,4′-BPDA (a-BPDA), and PEPA as shown in Fig. 2, and the calculated molecular weight (Mw) was 1560 g/mol. The detailed procedure of imide oligomer synthesis is described elsewhere [18, 19]. The Tri-A PI is commercially available as UPILEX-AD™.

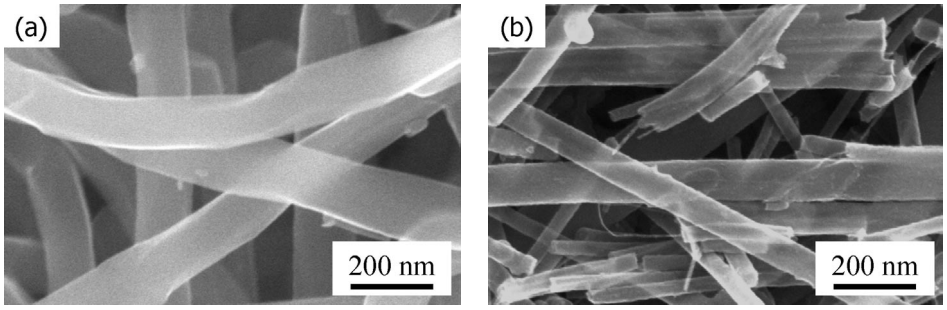

Figure 1. SEM micrographs of vapor grown carbon nanofibers (VGCF) and multi-walled carbon nanotubes (MWNT); (a) VGCF (Showa Denko KK., Japan), (b) MWNT (FT grade, CNRI Inc., Japan).

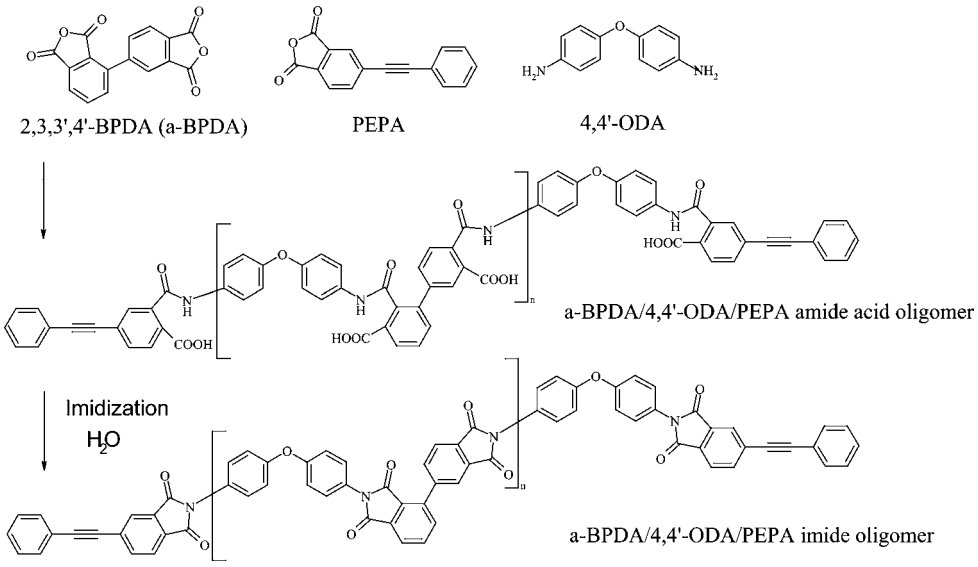

Figure 2. Synthetic scheme of the imide oligomers from the reaction of a-BPDA, 4,4′-ODA, and PEPA.

2.2. Composite preparation

VGCF/imide oligomer mixtures containing 0, 3.2, 7.7, and 14.3 wt% VGCF were prepared using a mechanical blender without any solvent (dry condition) for several minutes. The volume fractions of VGCFs are calculated to be 2.1, 5.2, 9.8 vol% from the density of the CNTs (2.0 g/cm^3) and the cured polyimide (1.31 g/cm^3). Particle size of the imide oligomers was in the range of 0.1–10 μm. There was no significant loss of aspect ratio during the mechanical blending, so the VGCFs were flexible enough for the mechanical blend process with the imide oligomers. The VGCF/imide oligomer mixture was melted at 320°C for 10 min on a steel plate in a hot press, and then cured at 370°C for 1 h under 0.2 MPa of pressure with PTFE

spacer (thickness 1 mm). This process is the same as that for the MWNT/Tri-A PI composites.

2.3. Characterizations

Rheological behaviors of nanofiber (VGCF or MWNT)/imide oligomer mixtures were characterized using an AR2000 rheometer (TA Instruments, USA). The measurements were carried out in an oscillatory shear mode using a parallel plate geometry (25 mm diameter, 2 mm gap width) from 200 to 400°C at 4°C/min with frequency of 1 Hz, and nominal strain of 0.1%.

The nanofiber dispersion of the composites was observed using an optical microscope. In order to characterize the thermomechanical properties, composites with different nanofiber concentrations were tested with a dynamic mechanical thermal analyzer (DMA). A TA Instruments Q800 was used in the single cantilever beam test mode with 17.5 mm span length, 5 mm width, and 1 mm thickness. The tests were run from 30°C to 450°C at 3°C/min with cycling rate of 1 Hz, and strain of 0.1%.

Tensile tests were conducted on a servo-hydraulic testing machine (Model 8501, Instron, USA) under a constant displacement rate of 0.5 mm/min at room temperature in order to evaluate the strength as well as the elastic modulus of the composites. GFRP end tabs (20 mm length, 2 mm thickness) were bonded on both sides of the grip portions. The specimen size was of 1 mm thickness, 5 mm width, and 80 mm overall length, and three specimens were tested. Longitudinal strain was measured using a contact type extensometer (Instron, USA) with a gage length of 12.5 mm.

Electrical impedance was measured using an LCR meter (Model 3522-50, Hioki E. E. Corp., Japan) from 10 Hz to 100 kHz under the peak electrical current of 1 mA. The specimen size was of 1 mm thickness, and 5 mm square, and electrical impedances were measured through the thickness (1 mm). Electrodes were formed on the surfaces using silver paste.

3. RESULTS AND DISCUSSION

3.1. Rheological behavior of powder mixtures

Dynamic viscosities, $|\eta^*|$, of the pure Tri-A PI oligomer, VGCF/Tri-A PI and MWNT/Tri-A PI mixtures, are shown in Figs 3 and 4, respectively. The relationship between minimum melt viscosity and nanofiber concentration is plotted in Fig. 5. The melt viscosities increase with nanofiber concentration, and such an increase of the VGCF/Tri-A PI mixtures is more significant than that of the MWNT/Tri-A PI mixtures. The viscosities of the 14.3 wt% CNF/Tri-A PI mixture increase to 4 orders for VGCFs, and 3 orders for MWNTs as compared to that of the pure imide oligomer. The melt viscosity seems to be saturated for above 15 wt% of VGCF addition, because the melt viscosity will become closed to that of the cured polymer. Neither thixotropy nor rheopexy were observed clearly.

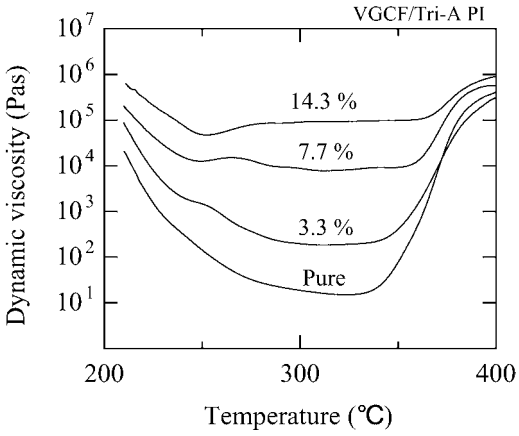

Figure 3. Dynamic viscosities of the VGCF/Tri-A PI imide oligomer mixtures.

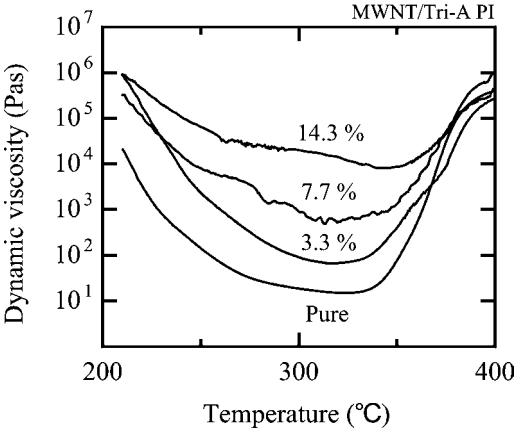

Figure 4. Dynamic viscosities of the MWNT/Tri-A PI imide oligomer mixtures.

The minimum melt viscosity of PETI-5 was reported to be approximately 1000 Pa.s at 340°C [23]; this value is almost same as that of the MWNT 10 wt%/Tri-A PI composite. Therefore, the melt viscosity of MWNT/Tri-A PI is low enough to apply composite matrix resin. The experimental result also suggests that VGCF/MWNT can be used to control the melt viscosity of the imide oligomer.

3.2. Microscopic observations

Figure 6a and b, shows optical micrographs of the VGCF (7.7 wt%)/Tri-A PI and MWNT (7.7 wt%)/Tri-A PI composites, respectively, after curing. The nanofibers just below the surfaces could be observed through the transparent polyimide under a dark image field. Dispersion of nanofibers is almost uniform, and remarkable aggregations were not observed in micron scale. It seemed that the nanofibers

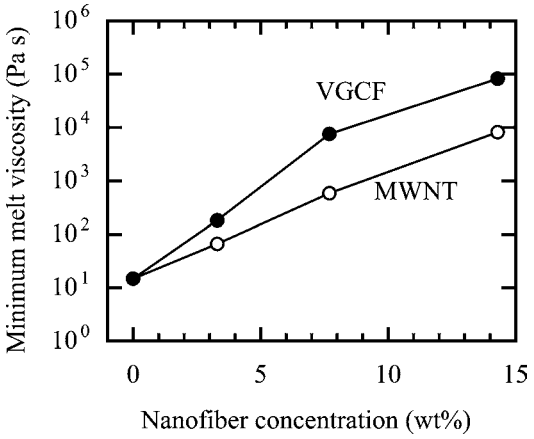

Figure 5. Minimum melt viscosities of the nanofibers/Tri-A PI imide oligomer mixtures as a function of nanofiber concentration.

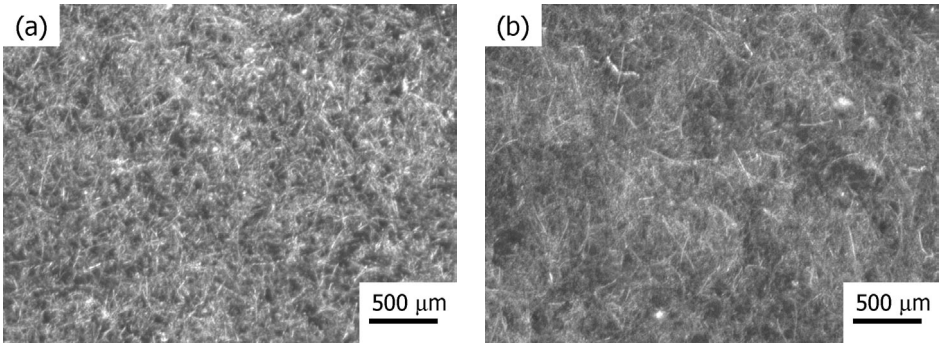

Figure 6. Optical micrographs of the nanofibers/Tri A-PI composites (Dark field image); (a) VGCF 7.7 wt%, (b) MWNT 7.7 wt%.

dispersed in a composite formed secondary network structures with sub-micron-order in addition to primary crosslink structure made of the polyimide.

3.3. Dynamic mechanical properties

The DMA curves (storage modulus E', loss modulus E'', and the tan δ) of the VGCF (14.3 wt%)/Tri-A PI and MWNT (14.3 wt%)/Tri-A PI composites are represented in Fig. 7 and Fig. 8, respectively. The glass transition temperatures (T_g) defined as the onset temperature of decrease in the storage modulus E' were summarized in Fig. 9 as a function of nanofiber loading. An increase in T_g and E' with the incorporation of the MWNTs was clearly observed. For example, the T_g of the 14.3 wt% MWNTs/Tri-A PI composite was 357°C, which was higher than that of the cured polyimide by 24 degrees. It was supposed that a secondary network structure was formed by the nanotubes in addition to the primary crosslink structure of the polymers, and the nanotubes immobilize polymer chains at elevated temperatures.

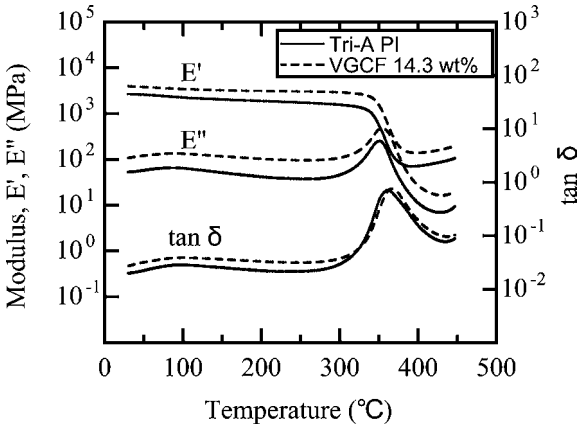

Figure 7. Dynamic mechanical traces of the VGCF (14.3 wt%)/Tri A-PI composites.

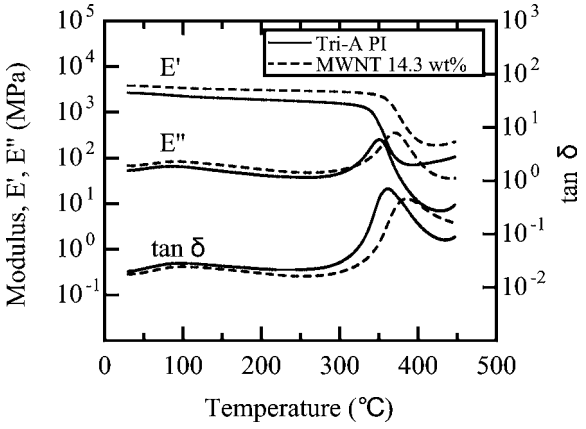

Figure 8. Dynamic mechanical traces of the MWNT (14.3 wt%)/Tri A-PI composites.

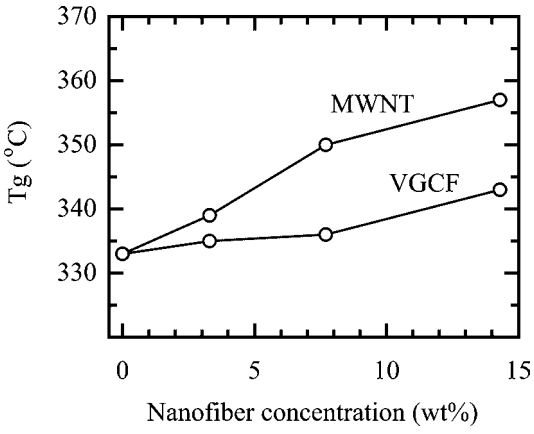

Figure 9. Glass transition temperature T_g *versus* nanofiber concentration.

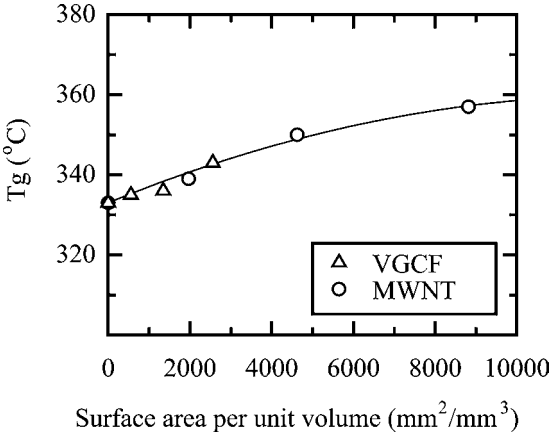

Figure 10. Glass transition temperature T_g *versus* nanofiber surface areas per unit volume.

On the other hand, the increase in T_g of the VGCF/Tri-A PI composites was not pronounced as compared to the MWNT/Tri-A PI composites, e.g. T_g increased only by 10 degrees for 14.3 wt% VGCF dispersion. Furthermore, the increase in T_g was not observed for carbon fiber reinforced/Tri-A PI composites [23].

Figure 10 shows the relationship between T_g and the surface area of the nanofibers per unit volume in the composites. Surface areas per unit volume (S_{pv}) were calculated using the specific surface area of the nanofibers (S_p), nanofiber volume fraction (V_f), and the nanofiber density (ρ_f) as follows;

$$S_{pv} = S_p V_f \rho_f. \tag{1}$$

The specific surface area was obtained from the nanofiber suppliers to be 15 m^2/g for the VGCF, and 45 m^2/g for the MWNT. A simple relation between T_g and surface areas was found. The experimental results suggest that there is interaction between the polyimide and nanofibers, and the interaction is strongly affected by surface areas of the nanofibers per unit volume in the composites. These chemical and physical interactions contribute to the immobilization of the polyimide chains at elevated temperatures, resulting in an increase in T_g.

3.4. Tensile properties

The longitudinal elastic moduli (Young's moduli), which were taken over the range of 0.1 to 0.3% strain, are shown in Fig. 11 as a function of nanofiber concentration. Compared to the base polymer, the elastic moduli of the nanofiber composites increased slightly with an addition of nanofibers (e.g. 37% increase for 14.3 wt% nanofiber dispersion). The elastic moduli of the VGCF composites were almost the same as those of the MWNT composites.

Qian *et al.* characterized MWNT/polystyrene (PS) composites with the addition of 1 wt%, and achieved about a 36–42% increase in the elastic modulus and a 25% increase in the tensile strength [5]. They estimated the elastic modulus of the

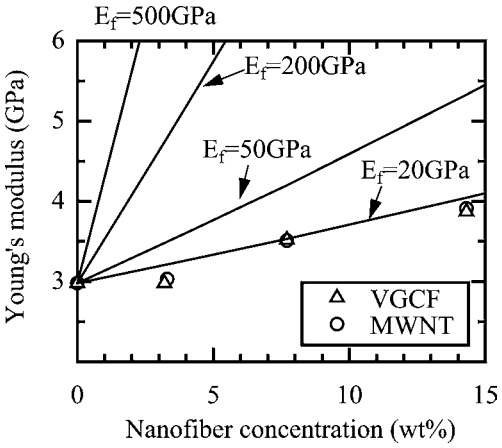

Figure 11. Effect of the nanofiber volume fraction on Young's modulus of the nanofibers/Tri-A PI composites.

composites using an in-plane random oriented discontinuous fiber lamina model as follows:

$$E = \left[\frac{3}{8}\left(\frac{1 + 2(l_f/d_f)\eta_L V_f}{1 - \eta_L V_f}\right) + \frac{5}{8}\left(\frac{1 + 2\eta_T V_f}{1 - \eta_T V_f}\right)\right] E_m, \tag{2}$$

$$\eta_L = \frac{(E_f/E_m) - 1}{(E_f/E_m) + 2(l_f/d_f)}, \quad \eta_T = \frac{(E_f/E_m) - 1}{(E_f/E_m) + 2}, \tag{3}$$

where E represents Young's modulus, l_f is the length, and d_f is the diameter of the nanotube. The aspect ratio ((l_f/d_f) term) of the nanotube is much higher than 10^2, so this term does not affect the estimated elastic modulus significantly. The elastic modulus was calculated using this equation, and numerical curves are superimposed in Fig. 11. The best fit elastic modulus of the nanofibers was 20 GPa, which is much lower than the values reported for isolated carbon nanotubes (>300 Pa) [24, 25]. Therefore, it is supposed that the stress transfer between the matrix and nanofibers is weak because of debonding and sliding at the interfaces between the nanofiber and matrix or at the interlayer of carbon nanotubes [26].

The average tensile properties such as elastic modulus E, ultimate tensile strength σ_{uts}, and failure strain $\varepsilon_{\max}$ are summarized in Table 1. In this study, an addition of VGCF/MWNT results in a decrease in the failure strain by 35–65% as compared to the base polymer. On the other hand, the failure strengths decrease by 15–30% by VGCF/MWNT addition because of the balance of elastic modulus and failure strain. It is known that the strength of nanofiber composites is strongly affected by microscopic defects such as the voids and nanofiber aggregation. The failure strain degradation with nanofiber addition is due to nanofiber aggregations in the composites. The detailed discussion was made elsewhere [17].

Table 1.
Properties of the VGCF/MWNT Tri A-PI composites

Filler	Filler concentration		T_g*	E**	σ_{uts}	ε_{max}
	(wt%)	(vol%)	(°C)	(GPa)	(MPa)	(%)
—	0	0	333	2.98	115.6	7.6
VGCF	3.2	2.1	335	2.98	81.6	3.8
	7.7	5.2	336	3.52	95.6	4.4
	14.3	9.8	343	3.87	94.8	5.0
MWNT	3.3	2.3	339	3.07	99.5	4.0
	7.7	5.4	350	3.28	97.6	3.6
	14.3	10.3	357	3.90	95.2	2.6

* Onset temperature of decreasing in storage modulus (DMA).
** Strain range of 0.1–0.3% (Tensile testing).

3.5. Electrical impedance

Figure 12 shows the electrical resistivity of the composites as a function of nanofiber concentration at 1 kHz, 1 mA. An electrical percolation model has been often applied for nanotubes/nanofiber composites as follows [4, 16];

$$\rho_{composite} = \rho_0(\phi - \phi_{th})^{-t}, \tag{4}$$

where $\rho_{composite}$ and ρ_0 are the electrical resistivities of the composite and of the filler, and ϕ_{th} is the threshold volume fraction of the fillers. When the filler volume fraction exceeds the percolation threshold, a conductive path is formed due to the interconnected fillers. The results of the least-square fit are $\rho_0 = 0.128\ \Omega\,\text{cm}$, $\phi_{th} = 2.2$ vol%, $t = 2.54$ for the MWNT composite, and $\rho_0 = 0.15\ \Omega\,\text{cm}$, $\phi_{th} = 1.0$ vol%, $t = 1.85$ for the VGCF composite. Fitting curves are superimposed on Fig. 12. The percolation threshold values are almost the same as that for a MWNT/epoxy composite [11], and lower than that for a VGCF/polypropylene (PP) composite [4]. This percolation threshold of MWNT composites is a higher than that of VGCF composites. It is known that high aspect ratio and large diameter of nanofibers allow reaching this threshold with a small nanofiber fraction [11, 16]. Therefore, VGCF dispersion is more effective in reducing electrical resisitivity than MWNT dispersion.

4. CONCLUSION

In this study, vapor grown carbon nanofibers (VGCF) were dispersed throughout a phenylethynyl terminated polyimide TriA-PI. The resulting composites containing 3.2, 7.7, 14.3 wt% VGCF exhibited relatively good dispersion. Tensile tests on the composites showed a slight increase in the elastic modulus and decrease in the failure stress and strain. Dynamic mechanical analyses (DMA) showed an increase in the glass transition temperature (T_g) with incorporation of VGCF; however, the increase in T_g was not pronounced as compared to MWNT dispersion.

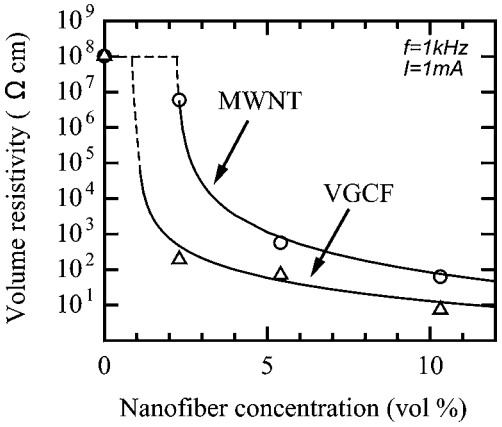

Figure 12. Electrical impedance of the VGCF/MWNT Tri-A PI composites at 1 kHz, 1 mA.

The experimental result suggested that nanofibers are immobilizing the polyimide chains at elevated temperatures, and the chemical and physical interactions between nanofibers and polyimide are governed by the surface area of the nanofibers per unit volume in composites.

Acknowledgements

The authors wish to sincerely thank Mr. Subiantro of CNRI Inc., Mr. Tsutomu Masuko of Showa Denko KK, and Mr. Hideki Ozawa of Ube Industries Ltd. for supplying starting materials. Ms. Masami Abe of the University of Electro-Communications assisted with sample preparation.

REFERENCES

1. E. T. Thostenson, Z. Ren and T.-W. Chou, Advances in the science and technology of carbon nanotubes and their composites: a review, *Compos. Sci. Technol.* **61**, 1899–1912 (2001).
2. K.-T. Lau and D. Hui, The revolutionary creation of new advanced materials — carbon nanotubes composites, *Composites: Part B* **33**, 263–277 (2002).
3. W. Brandl, G. Marginean, V. Chiria and W. Warschewski, Production and characterization of vapor grown carbon fiber/polypropylene composites, *Carbon* **42**, 5–9 (2004).
4. S. A. Gordeyev, F. J. Macedo, J. A. Ferreira, F. W. J. van Hattum and C. C. Bernardo, Transport properties of polymer-vapour grown carbon fibre composites, *Physica B* **279**, 33–36 (2000).
5. D. Qian, E. Co. Dickey, R. Andrews and T. Rantell, Load transfer and deformation mechanisms in carbon nanotubes-polystyrene composites, *Appl. Phys. Lett.* **76**, 2868–2870 (2000).
6. Z. Jia, Z. Wang. C. Xu, J. Liang, B. Wei, D. Wu and S. Zhu, Study on poly(methyl methacrylate)/carbon nanotube composites, *Mater. Sci. Eng*. **A271**, 395–400 (1999).
7. C. Stephan, T. P. Nguyen, M. L. de la Chapelle, S. Lefrant, C. Journet and P. Bernier, Characterization of single-walled carbon nanotubes-PMMA composites, *Synthetic Metals* **108**, 139–149 (2000).
8. C. A. Cooper, D. Ravich, D. Lips, J. Mayer and H. D. Wagner, Distribution and alignment of carbon nanotubes and nanofibrils in a polymer matrix, *Compos. Sci. Technol.* **62**, 1105–1112 (2002).

9. J. Sandler, P. Werner, M. S. P. Shaffer, V. Demchuk, V. Altstadt and A. H. Windle, Carbon-nanofibre-reinforced poly(ether ether ketone) composites, *Composites: Part A* **33**, 1033–1039 (2002).
10. P. Potschke, T. D. Fornes and D. R. Paul, Rheological behavior of multiwalled carbon nanotubes/polycarbonate composites, *Polymer* **43,** 3247–3255 (2002).
11. A. Allaoui, S. Bai, H. M. Cheng and J. B. Bai, Mechanical and electrical properties of a MWNT/epoxy composite, *Compos. Sci. Technol*. **62**, 1993–1998 (2002).
12. A. Eitan, L. S. Schadler, J. Hansen, P. M. Ajayan, R. W. Siegel, M. Terrones, M. Grobert, M. Reyes-Reyes, M. Mayne and H. Terrones, Processing and thermal characterization of nitrogen doped MWNT/Epoxy composites, in: *Proc. 10th US–Japan Conf. Composite Materials*, pp. 634–640 (2002).
13. T. Prasse, J.-Y. Cavaille and W. Bauhofer, Electric anisotropy of carbon nanofiber/epoxy resin composites due to electric field induced alignment, *Comp. Sci. Technol.* **63**, 1835–1841 (2003).
14. J. Sandler, M. S. P. Shaffer, T. Prasse, W. Bauhofer, K. Schulte and A. H. Windle, Development of a dispersion process for carbon nanotubes in an epoxy matrix and the resulting electrical properties, *Polymer.* **40**, 5967–5971 (1999).
15. K. A. Watson, J. G. Smith, Jr. and J. W. Connell, Space durable polyimide/carbon nanotubes composite films for electrical charge mitigation, in: *Proc. 48th Intern. SAMPE Symposium*, pp. 1145–1154 (2003).
16. Z. Ounaies, C. Park, K. E. Wise, E. J. Siochi and J. S. Harrison, Electrical properties of single wall carbon nanotubes reinforced polyimide composite, *Compos. Sci. Technol*. **63**, 1637–1646 (2003).
17. T. Ogasawara, Y. Ishida, R. Yokota and T. Ishikawa, Characterization of Multi-walled Carbon Nanotube/Phenylethynyl Terminated Polyimide Composites, *Composites: Part A* **35**, 67–74 (2004).
18. R. Yokota, S. Yamamoto, S. Yano, T. Sawaguchi, M. Hasegawa, H. Yamaguchi, H. Ozawa and R. Sato, Molecular design of heat resistant polyimides having excellent processability and high glass transition temperature, *High Performance Polymers* **13**, S61–S72 (2001).
19. R. Yokota, S. Yamamoto, S. Yano, T. Sawaguchi, M. Hasegawa, H. Yamaguchi, H. Ozawa and R. Sato, Novel phenylethynyl-terminated asymmetric BPDA based polyimides having excellent processability and thermo-oxidative stability, *Polyimides and Other High Temperature Polymers* **1**, 101–111 (2001).
20. P. M. Hergenrother and J. G. Smith, Jr., Chemistry and properties of imide oligomers end-capped with phenylethynylphthalic anhydrides, *Polymer* **35** (22), 4857–4864 (1994).
21. M. Endo, Y. A. Kim, T. Hayashi, K. Nishimura, T. Matusita, K. Miyashita and M. S. Dresselhaus, Vapor-grown carbon fibers (VGCFs) basic properties and their battery applications, *Carbon* **39** (9), 1287–1297 (2001).
22. Technical data sheet of vapor phase carbon fiber (VGCF™), Showa Denko KK., http://www.sdk.co.jp/contents_e/product/index.htm
23. T. Ogasawara, T. Ishikawa, R. Yokota, H. Ozawa, M. Taguchi, Y. Shigenari and K. Miyagawa, Processing and properties of carbon fiber reinforced Triple-A polyimide (Tri-A PI) matrix composites, *Adv. Composite Mater*. **11** (3), 277–286 (2002).
24. J.-P. Salventat, G. A. D. Briggs, J.-M. Bonard, R. R. Bacsa, A. J. Kulik, T. Stockli, N. A. Burnham and L. Forro, Elastic and shear moduli of single-walled carbon nanotubes ropes, *Phys. Rev. Lett.* **82** (5), 944–947 (1999).
25. M.-F. Yu, B. S. Files, S. Arepalli and R. S. Ruoff, Tensile loading of ropes of single wall carbon nanotubes and their mechanical properties, *Phys. Rev. Lett*. **84** (24), 5552–5555 (2000).
26. K.-T. Lau, M. Chipara, H.-Y. Ling and D. Hui On the effective elastic moduli of carbon nanotubes for nanocomposite structures, *Composites: Part B* **35**, 95–101 (2004).